Journal of Biomolecular NMR (2006) 34: 63–73
DOI 10.1007/s10858-005-5359-z

Article

Assignment strategy for fast relaxing signals: complete aminoacid identification in thulium substituted Calbindin D_{9K}

Stéphane Balayssac, Beatriz Jiménez & Mario Piccioli*
Department of Chemistry, Magnetic Resonance Center (CERM), University of Florence, Via Luigi Sacconi 6, 50019, Sesto Fiorentino, Florence, Italy

Received 28 June 2005; Accepted 14 November 2005

Key words: ^{13}C & ^{15}N direct detection, NMR spectroscopy, paramagnetic NMR, pseudo-contact shifts, sequence specific assignment, solution structure determination

Abstract

Paramagnetic proteins generally contain regions with diverse relaxation properties. Nuclei in regions far from the metal center may behave like those in diamagnetic proteins, but those closer to the metal experience rapid relaxation with accompanying line broadening. We have used a set of NMR experiments optimized to capture data from these various concentric regions in assigning the signals from a paramagnetic Calbindin D_{9K} derivative in which one of the two calcium ions has been replaced by thulium(III). Normal double- and triple-resonance experiments with ^{1}H detection were used in collecting data from nuclei in the diamagnetic-like region; these approaches identified signals from fewer than 50% of the amino acid residues (those with $d > 17.5$ Å from thulium(III)). Paramagnetism-optimized two-dimensional NMR experiments with ^{1}H detection were used in collecting data from nuclei in the next nearer region ($d > 15$ Å). Standard ($d > 14$ Å) and optimized ($d > 9$ Å) ^{13}C direct-detection experiments were used to capture data from nuclei in the next layer. Finally nuclei closest to the metal were detected by one-dimensional ^{13}C ($d > 5$ Å) and one-dimensional ^{15}N data collection ($d > 4.2$ Å). NMR signals were assigned on the basis of through-bond correlations and, for signals closest to the metal, pseudocontact shifts. The latter were determined from chemical shift differences between assigned signals in thulium(III) and lanthanum(III) derivatives of Calbindin D_{9K} and they were interpreted on the basis of a structural model for the lanthanide-substituted protein. This approach yielded assignments of at least one resonance per amino acid residue, including those in the thulium(III) coordination sphere.

Introduction

The interaction between nuclear spins and unpaired electron spins (hyperfine interaction) affects the NMR parameters. In the presence of a suitable paramagnetic center the consequences of this interaction can be translated into paramagnetism-based constraints for structural calculations: pseudocontact shifts, *pcs* (Banci et al., 1996), residual dipolar couplings, *rdc* (Tolman et al., 1995), cross correlation rates, *ccr* (Hus et al., 2000; Déméné et al., 2000; Bertini et al., 2002b), and relaxation rate enhancements, R_1^{para} and R_2^{para} (Bertini et al., 1996). However, the effects of the hyperfine interaction dramatically reduce the intensity of NOE's and the coherence transfer efficiency in homo- and heteronuclear experiments, thus preventing signal identification, spectral assignment and structural determination through standard approaches.

In the last years, a methodology was developed to obtain sequence specific assignments via ^{13}C

*To whom correspondence should be addressed. E-mail: piccioli@cerm.unifi.it

direct detection (Bertini et al., 2004a; Bermel et al., 2005a, b). The small magnetic moment of the heteronuclei (^{13}C, ^{15}N), makes this methodology valuable to overcome the limits given by fast ^{1}H relaxation (Bertini et al., 2001c) and, indeed, it has been successfully applied to paramagnetic proteins (Wilkens et al., 1998; Machonkin et al., 2002; Arnesano et al., 2003; Babini et al., 2004; Bertini et al., 2004b; Machonkin et al., 2004; Bertini et al., 2005).

The rationale behind the success of lanthanides as shift reagents lies in their peculiar electronic properties (Kurland and McGarvey, 1970; Bleaney, 1972; Allegrozzi et al., 2000). These metals are characterized by low-lying excited levels that produce strong spin–orbit couplings and short electronic relaxation correlation times, τ_s. A consequence of the strong spin–orbit coupling is the large magnetic susceptibility anisotropy which, in turn, generates large *pcs*; a consequence of short τ_s is the small contribution to line broadening due to dipole–dipole coupling, so that transverse relaxation is dominated by the Curie spin term. The magnetic susceptibility anisotropy varies up to one order of magnitude when passing from one ion of the series to another (Allegrozzi et al., 2000) because it depends on J, a vectorial combination of spin and orbital angular moments. Metal ions with large magnetic anisotropies, like Tb^{3+}, Tm^{3+} or Dy^{3+} (Bleaney, 1972; Bertini et al., 2001b, d) provide *pcs* up to 30–40 Å away from the metal center and are therefore a source of long-range structural constraints. Due to their large J values, these metals also provide the largest contributions to paramagnetism-induced line broadening. Coherence transfer among nuclei can thus be quenched and, eventually, the NMR signals can be broaden beyond detection.

The efficiency of ^{13}C direct detection in paramagnetic metalloproteins to move the detectability threshold close to the metal center has been recently addressed, using a combination of dipolar and scalar experiments (Babini et al., 2004). Here we report in detail the assignment strategy based only on scalar coupling experiments. Additionally, we show here that ^{15}N direct detection is a unique tool, for a strong shift reagent such as Tm^{3+}, to obtain information in the first coordination sphere of the metal ion.

Our system of study is Calbindin D_{9K}, which is a di-calcium binding protein of 75 aminoacid (Kördel et al., 1993; Skelton et al., 1994) (Ca_2Cb, hereafter). The Ca^{2+} in site I remains unchanged (Vogel et al., 1985; Akke et al., 1991), while the one in site II could be easily exchanged with other metal ions like those belonging to the lanthanide series (Kretsinger, 1980; Akke et al., 1995). To obtain the long-range constraints, we have substituted the calcium(II) with thulium(III) (CaTmCb) at site II. Pseudocontact shifts were factorized using Calbindin lanthanum(III) derivative (CaLaCb) as a diamagnetic reference.

Materials and methods

Sample preparation

Bovine Calbindin D_{9K} expressed in *Escherichia coli* (Brodin et al., 1986; Chazin et al., 1989; Malmendal et al., 1998) was purchased from ProtEra s.r.l. Previously reported protocols were used for protein purification (Johansson et al., 1990) and for preparing CaLaCb and CaTmCb (Allegrozzi et al., 2000).

NMR spectroscopy

NMR data sets were acquired at 300 K on Bruker Avance 400, 500, 700 and 900 spectrometers with magnets operating, respectively, at 9.4, 11.7, 16.4 and 21.1 T. All spectrometers were equipped with 5-mm probes with z-axis gradients. The 400 MHz probe was a broad band tuned to the direct acquisition of heteronuclei (BBO); the 500 MHz probe was a triple resonance ^{1}H cryoprobe with a cooled ^{13}C preamplifier (TCI); the 700 MHz probe was a triple resonance one in which the inner coil was optimized for the direct acquisition of ^{13}C (TXO); the 900 MHz probe was a standard triple resonance ^{1}H cryoprobe (CP-TXI).

In order to obtain sequence specific backbone assignments, a set of sensitivity-enhanced triple resonance experiments was performed, including HNCO (Kay et al., 1990), HNCA (Kay et al., 1990), CBCA(CO)NH (Grzesiek and Bax, 1992). In addition, ^{1}H,^{15}N-HSQC (Bodenhausen and Ruben, 1980), ^{1}H,^{15}N-NOESY-HSQC (Kay et al., 1989), and ^{1}H,^{13}C-HSQC data sets were collected, in order to aid backbone assignments procedure and alleviate possible ambiguities. The number of real points acquired were 256 for ^{15}N and ^{13}C in t_1

dimension and 1024 in acquisition (t_2 dimension). Raw data were multiplied by a squared cosine window function and Fourier transformed to obtain a final matrix of 1024×512. A polynomial baseline correction was applied in both dimensions. For all the above experiments, from 8 to 32 scans were collected, using a relaxation delay of 1 s.

The same experiments were also run by optimizing the parameters to observe fast-relaxing resonances. We decreased the usual INEPT transfer delays in ^{1}H,^{15}N-HSQC, ^{1}H,^{13}C-HSQC, HNCO, and CBCA(CO)NH (Gelis et al., 2003) to 1.3, 0.9, 0.9 and 0.7 ms, respectively. Recycle delay was 300 ms. The number of scans was increased in order to have the same duration of the diamagnetic experiments.

^{13}C direct detection experiments: CC-COSY (Bertini et al., 2001c), CACO (Bermel et al., 2005a; Bertini et al., 2005), CBCACO (Bermel et al., 2005a) and CON (Kostic et al., 2002) were performed using Q5 Gaussian cascades (Emsley and Bodenhausen, 1992) of 333 μs length for 90° pulses, and Q3 Gaussian cascades of 220 μs for 180° pulses. A 50 μs rectangular pulse was used for $^{13}C'$ refocusing during $^{13}C^{\alpha}$ evolution period. Spectral windows of 40 ppm, 60/100 ppm and 40 ppm were used for the $^{13}C'$, $^{13}C^{\alpha}$ and ^{15}N dimensions using carrier frequencies at 175 ppm ($^{13}C'$), 53 ppm ($^{13}C^{\alpha}$), 39 ppm ($^{13}C^{\alpha}/^{13}C^{\beta}$) and 120 ppm ($^{15}N$). Real data point matrices were, respectively: 800 × 600 for the CACO-IPAP (Bermel et al., 2005a), 512 × 160 for the CACO-AP (Bertini et al., 2005), 1024 × 192 in the CBCACO and 512 × 600 in CON. The coherence transfer for $^{13}C'$–$^{13}C^{\alpha}$ coupling (typically $1/2J = 9.1$ ms) was shortened to 5.5 ms in the paramagnetic tailored experiments, while the one for $^{13}C^{\beta}$–$^{13}C^{\alpha}$ was 12.4 ms and the $^{13}C'$–^{15}N was 25 ms. TPPI (Marion and Wüthrich, 1983) was used to obtain quadrature detection in the indirect dimension. Both 1024 or 32 scans per fid were collected, using a recycle delay of 300 ms for paramagnetic optimized sequences and 1 s for the detection of diamagnetic signals. Spectral windows for the CC-COSY were both 300 ppm and the carrier was set at 150 ppm. A 2048 × 300 data point matrix was acquired using 512 scans each fid. Decoupling of ^{15}N and ^{13}C was performed using a garp4 pulse sequence (Shaka et al., 1985), while ^{1}H was decoupled using waltz-16 (Shaka et al., 1983).

1D ^{15}N was acquired at 40.54 MHz ^{15}N Larmor Frequency using a BBO probe, with 40 ms of relaxation delay. On average, 2–3 milion scans were collected to obtain a 1D spectrum. 1D ^{13}C spectrum was acquired at 175.03 MHz Larmor Frequency, using a TXO probe, with a recycle delay of 150 ms, spectral window of 300 ppm and 16 K scans.

All NMR data were processed with Bruker XWINNMR software package and analyzed using NEASY (Eccles et al., 1991), a tool of CARA (http://www.nmr.ch).

Determination of the magnetic susceptibility anisotropy tensor

The paramagnetic susceptibility tensor, $\chi^{\mathbf{para}}$, can be obtained from the fitting of the *pcs* values, according to (McConnell and Robertson, 1958; Banci et al., 1996):

$$\delta_i^{pc} = \frac{1}{12\pi r_i^3}\left[\Delta\chi_{\mathrm{ax}}(3\cos^2\theta - 1) + \frac{3}{2}\Delta\chi_{\mathrm{rh}}\left(\sin^2\theta\cos 2\phi\right)\right] \quad (1)$$

where $\Delta\chi_{\mathrm{ax}}$ and $\Delta\chi_{\mathrm{rh}}$ are the axial and rhombic components of the $\chi^{\mathbf{para}}$, θ_i and ϕ_i are the spherical polar angles of atom i with respect to the principal axes of the $\chi^{\mathbf{para}}$ centered on the metal ion, and r_{i} is the distance between atom i and the metal ion. The experimental *pcs* were obtained from the observed chemical shifts of CaTmCb subtracting those of the CaLaCb (its diamagnetic homolog). The difference in chemical shift is equal to the *pcs* for those nuclei belonging to residues not directly bound to the metal, for which contact contribution can not be neglected. The tensor parameters were obtained with the program FANTASIAN (Banci et al., 1997) (available from http://www.postgenomicnmr.net) which optimizes the fit of the experimental *pcs* values over the given structure. The structure used for the refinement steps was 1KQV.pdb (Bertini et al., 2001a). It corresponds to the 30 best NMR structures of the cerium(III) monosubstituted P43M Calbindin D_{9K}. The paramagnetic susceptibility tensor components ($\Delta\chi_{\mathrm{ax}}$, $\Delta\chi_{\mathrm{rh}}$,θ_{i},ϕ_{i},r_{i}) have been used to calculate the shifts of those resonances which do not show connectivities in order to complete the assignment.

Results

CaLaCb derivative

The substitution of Ca^{2+} with Ln^{3+} in calcium binding proteins is known to be isomorphic (Akke et al., 1995; Bertini et al., 2002a). However, as reported for other metalloproteins (Vathyam et al., 2000), charge effects (Sorkin and Miller, 2000; Miller et al., 2003), independent from paramagnetism, can affect chemical shifts in the first coordination sphere of the metal center. Therefore the CaLaCb derivative is the most appropriate diamagnetic reference (Bertini et al., 2001b).

For CaLaCb, 69 out of 72 ^{1}H,^{15}N-HSQC signals were previously assigned (Bertini et al., 2001b). We have now identified all backbone resonances using both ^{1}H and ^{13}C detection experiments. Additionally, all C^{β} signals but four residues (Lys 16, Leu 28, Phe 63, Lys 72) could be observed in a CBCACO experiment, as well as all C^{γ} and C^{δ} from carbonyl containing side chains. The complete available assignments for CaLaCb have been deposited in the BMRB, accession number 6699.

CaTmCb derivative

Sequence specific assignment

Standard ^{1}H,^{15}N- and ^{1}H, ^{13}C-HSQC spectra of CaTmCb are shown in Figure 1a and b. 33 and 38 backbone signals were respectively observed and assigned via HNCA, HNCO and CBCACONH experiments (data not shown). About 50% of the protein is, to some extent, affected by paramagnetism. Tailored versions of the same experiments revealed eight additional peaks in the ^{1}H, ^{15}N-HSQC and 13 peaks in the ^{1}H,^{13}C-HSQC (six

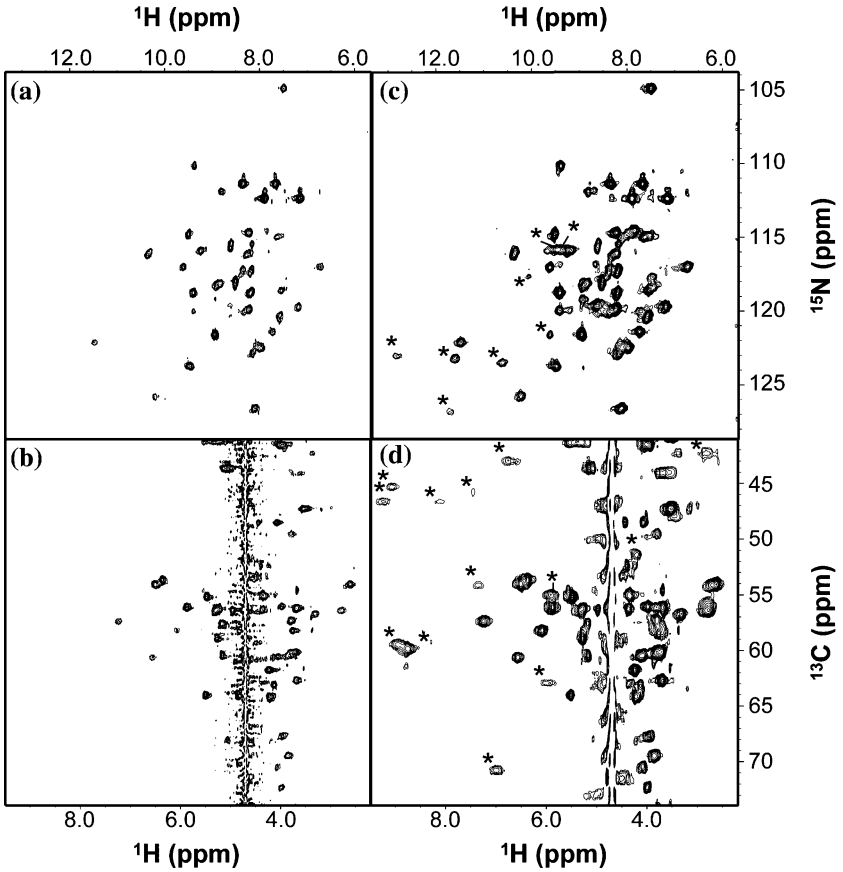

Figure 1. ^{1}H,^{15}N-HSQC spectra of CaTmCb sample recorded with (a) normal experimental conditions, (c) conditions optimized for paramagnetic systems. Analogous ^{1}H, ^{13}C-HSQC spectra are reported in (b) and (d), respectively. Few additional peaks are observed in (c) and (d). They are indicated by asterisks. Experiments were performed on a 900 MHz Bruker Avance spectrometer, at 300 K.

of which are C^{α}–H^{α}), as shown in Figure 1c and d, respectively and summarized in Table 1. A protocol previously proposed for ^{1}H NMR experiments optimized for paramagnetic proteins (Gelis et al., 2003) provided some additional sequence specific assignments. For six of the eight amide peaks observed in the ^{1}H, ^{15}N-HSQC spectrum (Figure 1c), a tailored HNCO gave connectivities to the C′ of the previous residue, which could be connected to the C^{α} via a CACO experiment (see below). Three of the above signals were therefore assigned to Glu 17, Met 43 and Leu 69 and, similarly, two peaks, only observed in the paramagnetic version of ^{1}H, ^{13}C-HSQC, were assigned to Ala 14 and Met 43. Overall, backbone assignment was possible only for 41 out of 75 aminoacids (Table 1), which are mostly located in helices I and II as shown in Figure 2. Missing cross peaks belong to residues 18–28 and 44–66 and the unobserved signals correspond to nuclei in the sphere 17.5 Å from the Tm^{3+} ion.

^{13}C and ^{15}N direct detection to identify new resonances

Figure 3 shows the CACO experiment, in both standard and paramagnetism-optimized versions. Forty-two signals could be observed in the diamagnetic spectrum (Figure 3a), whereas 17 additional peaks (12 corresponding to backbone resonances) were detected in the paramagnetic tailored experiment (Figure 3b). The two experiments are complementary, because resolution of sharper peaks is poorer in the paramagnetic version. Three backbone C^{α}–C′ and three C^{α}–C^{β} connectivities were also observed in the tailored CC-COSY and CBCACO (data not shown).

The 1D ^{13}C experiment, recorded with short recycle delays, revealed 23 additional signals (Figure 4a), with line widths between 125 and 600 Hz resonating in spectral regions where ^{13}C

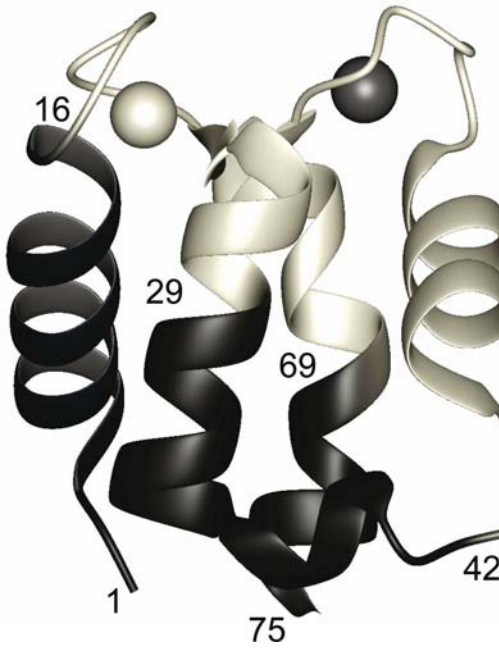

Figure 2. Cartoon representation of Calbindin D_{9K} solution structure (Bertini et al., 2001a). Tm^{3+} in loop II is colored medium grey. Residues shown in ivory escaped detection in standard diamagnetic HSQC experiments.

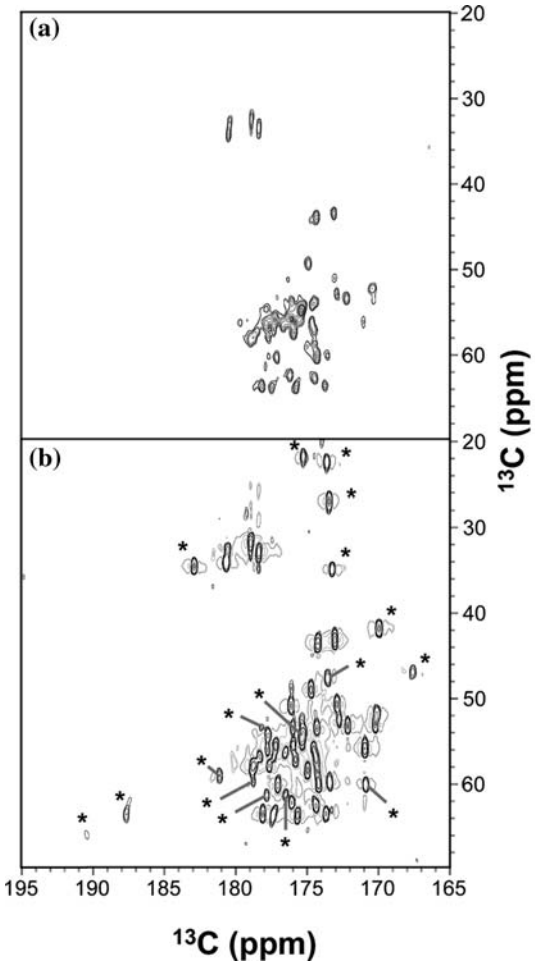

Figure 3. (a) CACO-IPAP and (b) CACO-AP spectra of CaTmCb. The additional peaks observed in (b) are indicated by asterisks. Both spectra were acquired using a Bruker Avance 700 spectrometer equipped with TXO probe, at 300 K.

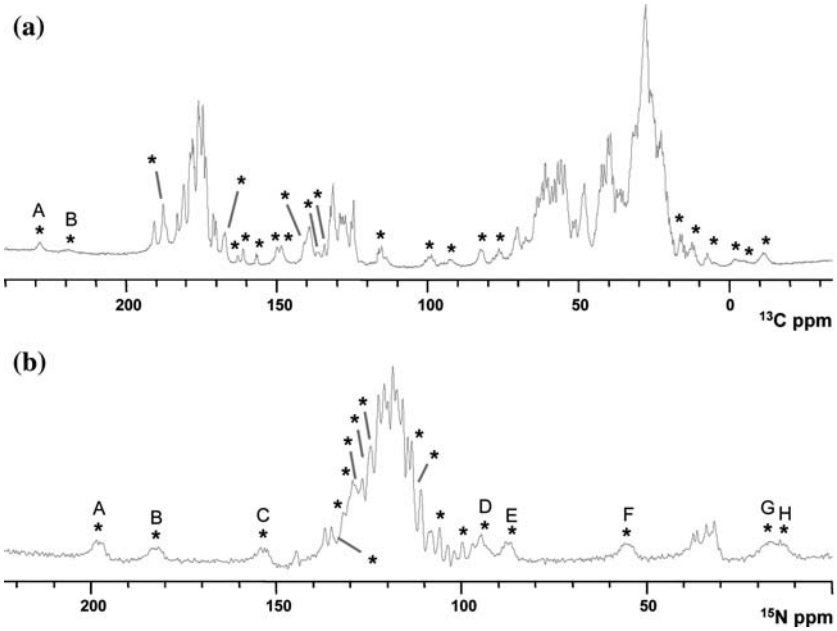

Figure 4. (a) ^{13}C 1D spectrum of CaTmCb, at 176.03 Hz, 300 K. (b) ^{15}N 1D spectrum of CaTmCb, at 40.54 MHz. Signals that could be observed only in 1D spectra are indicated by asterisks.

Table 1. Number of backbone cross peaks observed in different experiments

	^{1}H, ^{15}N-HSQC	^{1}H$^{\alpha}$, ^{13}C$^{\alpha}$-HSQC	CACO
Standard	33	38	42
Relaxation-optimized	41	44	54

signals are not expected. These were found to correspond to signals with large *pcs* values. No signal from these nuclei could be observed in CC-COSY or in CACO experiments as expected for resonances of nuclei which are about 5 Å away from the metal ion (Bertini et al., 2001d).

In the ^{15}N spectrum of CaTmCb, reported in Figure 4b, 18 resonances that completely escaped detection in the ^{1}H, ^{15}N-HSQC experiment are clearly observed. As in the previous case, experiments based on coherence transfer are useless to assign these signals because scalar couplings between ^{15}N and ^{13}C spins are, by far, smaller than transverse ^{13}C relaxation.

Assignments based on pseudocontact shifts of heteronuclei

As summarized in Table 2, 237 *pcs* from CaTmCb were used in a first run to calculate the $\Delta\chi^{ax}$ and $\Delta\chi^{rh}$ and, in turn, to predict *pcs* for the whole protein. Overall, 51 nuclei of backbone and 17 nuclei of side chain were identified and their *pcs* used as additional input for a second FANTASIAN run. With the exception of three peaks in the ^{1}H–^{13}C HSQC experiment, most likely arising from side chains, all resonances indicated with asterisks in Figures 1 and 3 were assigned.

The broadest ^{13}C and ^{15}N signals observed in the 1D spectra can be assigned to covalent C′–N pairs by assuming that these should have very similar *pcs* values. We consider the two downfield shifted ^{13}C signals and, in the ^{15}N spectrum, the three largely downfield and five upfield shifted resonances (labeled A-H in Figure 4). Two pairs of signals, which are about 50 ppm downfield shifted with respect to the average of diamagnetic resonances are observed in both ^{15}N and ^{13}C spectra (A and B in both Figure 4a and b). Therefore, they are likely to originate from two C′–N groups. According to the FANTASIAN results, two candidates are C'_{53}–N_{54} and C'_{54}–N_{55}. Predicted *pcs* and line widths suggest that (Figure 4a) the broad signal B (220 ppm, 700 Hz), corresponds to C'_{54}, while the most shifted resonance A (230 ppm, and 340 Hz) can be assigned to C'_{53}. The assignment in the ^{15}N spectrum is performed accordingly (Figure 4b). The ^{15}N spectrum also shows another

Table 2. Type and number of assignments, based on pseudocontact shifts, during different FANTASIAN runs

	Assigned atoms						Tensor (10^{-32} m^3)		Assignments using FANTASIAN					
	H^N	N^H	C^α	H^α	C'	Other	$\Delta\chi_{ax}$	$\Delta\chi_{rh}$	H^N	N^H	C^α	H^α	C'	Other
1st run	33[a]	33[a]	38[a]	38[a]	35[a]	43[a]	−22.2	−20.7	5[c]	2[b]	4[c]	4[c]	3[b]	8[c]
	3[c]	2[b]	1[b]	2[c]	2[b]					5[c]	12[d]		1[c]	9[d]
		3[c]	2[c]		2[c]								15[d]	
2nd run	41	45	57	44	58	60	−23.5	−20.0		13[e]			6[e]	
3rd run	41	58	57	44	64	60	−20.9	−25.2						

On the left part of the table, number of *pcs*, for each atom type, used to calculate the tensor, whose values are reported in the central part. On the right side, numbers refers to the new atoms that could be assigned thanks to the comparison between experimental and predicted *pcs*.

[a] ^{1}H,^{15}N-HSQC, ^{1}H, ^{13}C-HSQC, HNCO, CBCA(CO)NH, HNCA.

[b] CACO-IPAP, CBCACO-IPAP, CON.

[c] ^{1}H,^{15}N-HSQC, ^{1}H, ^{13}C-HSQC, HNCO paramagnetic tailored version.

[d] CACO-AP, CBCACO-AP and CC-COSY paramagnetic tailored version.

[e] ^{15}N 1D, ^{13}C 1D experiments.

very broad and clearly shifted feature in the downfield region (signal C), which has the same linewidth as A and B. The only reasonable candidate is N_{61}, which is 4.5 Å away from the metal center and therefore it is expected to have the same transverse relaxation rate of N_{54} and N_{55}, with a predicted average *pcs* of about 20 ppm. Signal C has no counterpart in the ^{13}C spectrum; however, C'_{60} is directly bound to Tm^{3+} and therefore it may experience a substantial amount of contact shift and strong dipolar relaxation.

Nineteen signals were safely assigned and their *pcs* used to calculate a more refined magnetic anisotropy tensor (Table 2). The assignments for CaTmCb have been deposited in the BMRB, accession number 6697.

A tentative assignment for the observed upfield shifted resonances in the ^{15}N 1D spectrum (Figure 4b) can be proposed. Large and negative *pcs* values, from −30 to more than −100 ppm, are predicted for N_{57}, N_{58} and N_{59}. These values are compatible with the assignment of each of the resonances F-H. A similar situation holds for peaks D-E. *Pcs* in the range −20/−60 ppm are predicted for N_{56} and N_{60}, but they could not be assigned unambiguously.

Discussion

The ensemble of results described above is summarized in Table 3. On the one hand, when τ_s of the paramagnetic ion is such that the effects induced by the metal merely affect a relatively small sphere, the optimization of ^{1}H detected experiments is sufficient to give information even in the proximity of the metal center (Vila and Fernández, 1996; Donaire et al., 1998; Donaire et al., 2001). On the other hand, if the loss due to the paramagnetic ion affects about 50% of protein residues, the contribution provided by optimized ^{1}H detected experiments is relatively small and insufficient to provide a substantial improvement of the available assignments. Within this framework, the CACO experiments have been shown here to be a quite powerful tool to recognize residues that would have been unobserved.

There is a strong synergism between ^{1}H tailored and ^{13}C detected experiments. As observed in Table 3, all different experiments contribute to fill the gaps occurring in the assignment made with the standard approach (non-bolded notation). Optimized experiments usually are informative for one or two residues at the border region of diamagnetic assignments, as it is the case of residues 18 and 28 (Table 3) in the unassigned region 17–29. Then all C^α—C' residues of this loop could be observed in CACO-AP or in CC-COSY experiments, while ^{15}N 1D allows us to observe several signals in the loop binding the paramagnetic metal ion. The contribution of 1D experiments is essential to obtain structural constraints within loop II. We have assigned at least one resonance for each residue of the Tm^{3+} binding site.

Table 3. Backbone ^{1}H ^{15}N and ^{13}C resonance assignments for CaTmCb at 300 K and pH 6.0 (BMRB deposit has the accession number 6697)

Residue	N	H^N	C^α	H^α	C′
Lys 1	123.8	8.91	53.2	4.64	172.7
Ser 2	119.2	9.01	53.7	4.52	170.2
Pro 3	135.2[d]		62.8	4.13	176.1
Glu 4	117.3	8.27	56.8	3.30	176.6
Glu 5	121.4	7.84	56.0	3.73	176.9
Leu 6	119.9	8.32	54.9	3.70	175.3
Lys 7	120.2	7.63	56.5	2.77	174.5
Gly 8	104.9	7.57	44.1	3.75/3.59	174.2
Ile 9	122.4	8.06	63.1	3.67	174.4
Phe 10	120.1	8.45	60.4	3.74	173.4
Glu 11	114.6	7.93	56.5	3.30	175.6
Lys 12	118.6	7.64	55.9	3.68	175.4
Tyr 13	114.9	7.70	59.0	4.45	174.3
Ala 14	119.6	8.71	**51.5**[b,e]	**4.18**[b]	176.1
Ala 15	116.9	6.79	49.6	3.79	174.7
Lys 16	119.7	7.29	57.4	3.79	**174.4**[c,d]
Glu 17	**115.9**[a,c,d]	**9.56**[a]	**51.3**[e]		**172.9**[e]
Gly 18	**113.1**[h]		**42.4**[b,f]	**3.34/2.80**[b]	**170.0**[f]
Asp 19			**48.3**[f]		**173.6**[f]
Pro 20	**134.5**[h]		**60.7**[f]		**170.9**[f]
Asn 21			**47.6**[f]		**167.6**[f]
Gln 22	**112.6**[h]		**49.5**[g]		**171.5**[g]
Leu 23	**128.8**[h]		**54.3**[b,f]	**7.31**[b]	**178.2**[f]
Ser 24			**56.2**[f]		**176.0**[f]
Lys 25			**61.7**[f]		**177.8**[f]
Glu 26					**178.4**[d]
Glu 27	**121.5**[d]		**58.6**[f]		**178.8**[d,f]
Leu 28	**123.0**[a,c,d]	**12.92**[a]	**59.5**[b,e]	**8.73**[b]	**178.8**[d,e]
Lys 29	**123.2**[a,c,d]	**11.68**[a]	60.7	6.53	177.0
Leu 30	119.9	9.50	56.5	5.30	177.7
Leu 31	125.8	10.29	58.1	3.75	178.7
Leu 32	122.1	11.55	58.4	6.06	177.6
Gln 33	116.1	10.47	57.6	5.17	175.8
Thr 34	111.9	8.89	64.0	4.87	173.7
Glu 35	117.1	9.69	54.7	4.82	175.1
Phe 36	115.9	9.33	53.8	6.36	172.2
Pro 37	136.8[d]		64.1	5.50	178.1
Ser 38	114.8	9.59	59.0	5.27	174.9
Leu 39	123.7	9.57	55.9	5.87	177.3
Leu 40	118.8	9.49	54.1	6.50	176.0
Lys 41	121.5	9.04	55.0	5.47	175.3
Gly 42	110.2	9.46	43.8	5.14/5.05	173.0
Met 43	**121.0**[a,c,d]	**9.70**[a]	**54.6**[b,e]	**5.90**[b]	**175.5**[c,e]
Ser 44	**117.6**[a,c]	**10.15**[a]			
Thr 45	**115.3**[a]	**9.52**[a]			
Leu 46	**125.0**[h]				
Asp 47					
Glu 48			**59.6**[b,f]	**8.75**[b]	**181.1**[f]

Table 3. Continued.

Residue	N	H^N	C^α	H^α	C′
Leu 49	**126.8**[a]	**11.67**[a]	**64.3**[f]		**186.6**[f]
Phe 50	**127.5**[h]				**187.6**[i]
Glu 51	**124.5**[h]		**62.2**[g]		**183.1**[g]
Glu 52			**54.0**[f]		**190.6**[f]
Leu 53	**131.9**[h]				**228.5**[i]
Asp 54	**198.5**[h]				**219.0**[i]
Lys 55	**182.6**[h]				
Asn 56	**88.1/94.7**[h,j]				
Gly 57	**15.2/17.0/55.3**[h,j]				
Asp 58	**15.2/17.0/55.3**[h,j]				
Gly 59	**15.2/17.0/55.3**[h,j]				
Glu 60	**88.1/94.7**[h,j]				
Val 61	**153.2**[h]				
Ser 62					**161.1**[i]
Phe 63					**167.1**[i]
Glu 64	**105.9**[h]				**163.0**[i]
Glu 65	**99.8**[h]		**43.4**[g]		**176.0**[g]
Phe 66			**61.7**[f]		**176.5**[f]
Gln 67			54.2	2.61	**144.3**[d]
Val 68	**117.5**[d]		64.2	4.69	**177.4**[c,d]
Leu 69	**123.5**[a,c,d]	**10.69**[a]	57.3	7.24	177.3
Val 70	117.2	8.45	64.3	4.23	175.7
Lys 71	118.8	8.29	55.6	3.97	175.6
Lys 72	118.2	8.99	56.1	5.24	176.3
Ile 73	115.5	8.67	60.5	5.16	174.2
Ser 74	118.0	8.61	56.4	4.36	170.9
Gln 75	126.6	8.21	54.9	4.32	177.7[e]

Assignments written in roman type character were obtained using standard ^{1}H detected experiments. Those reported in bold characters refer to resonance revealed either by ^{1}H detected experiments optimized for the detection of paramagnetic signals or by ^{13}C or ^{15}N detected experiments. For each chemical shift value, the various experiments that allowed identification are reported.
[a] ^{1}H, ^{15}N-HSQC; [b] ^{1}H, ^{13}C-HSQC; [c] HNCO; [d] CON; [e] CACO-IPAP; [f] CACO-AP; [g] ^{13}C, CC-COSY; [h] ^{15}N 1D and [i] ^{13}C 1D carbon and nitrogen direct detection; [j]ambiguous assignments.

The low γ of ^{15}N permits the detection of signals from nuclei that are much closer to the metal center than those observed via ^{1}H or ^{13}C. The assignment of few ^{15}N resonances would allow the use of these constraints in a region in which structural restrictions are very scarce, if any. This finding is well known in theory, yet ^{15}N direct detection has been barely used, due to its low sensitivity (Wilkens et al., 1998; Xia et al., 1999; Machonkin et al., 2004; Caillet-Saguy et al. 2005).

Figure 5 visualizes the various substructure spheres available with the different approaches. ^{15}N direct detection observes resonances which are up to 4.2 Å close to the metal center. Remarkably, these signals could have never been assigned without the knowledge of accurate values of the χ^{para} due to the large number of available ^{13}C and ^{15}N *pcs*.

Conclusions

We have shown here that the optimization and simultaneous use of ^{1}H, ^{13}C and ^{15}N detected experiments disclose a number of resonances in close proximity of a paramagnetic center. Overall, the percentage of assigned protein signals was increased from 44 to 84% for ^{15}N, from 50 to 79% for $^{13}C^\alpha$ and from 44 to 85% for $^{13}C'$. A consistent set of experiments is required to achieve these results (Table 3). The number of residues in CaTmCb observed with standard

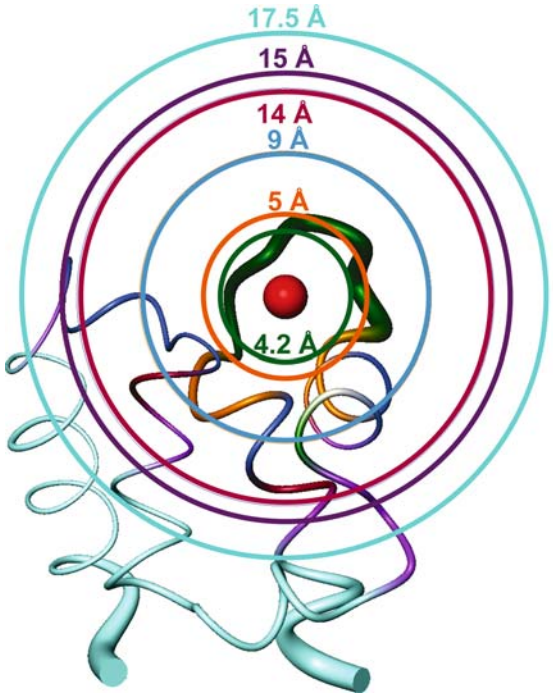

Figure 5. Schematic drawings of the blind spheres around Tm^{3+}. Aminoacids are coloured differently according to each set of NMR experiments: Up to 17.5 Å for standard ^{1}H detected NMR experiments (cyan), 15 Å for ^{1}H experiments optimized to paramagnetics (purple), 14 Å for "standard" ^{13}C detected experiments (brown), 9 Å for ^{13}C detected experiments optimized to paramagnetics (blue), 5 Å for ^{13}C 1D spectra (orange), 4.2 Å for 1D ^{15}N spectra (green).

approaches was only 50%. Now, with the unique exception of Asp 47, which is part of the flexible linker region in between the two EF-hand subunits, we have at least one resonance assigned for each of the 75 aminoacids. This opens the possibility to characterize also the first coordination environment when dealing with very efficient shift reagents.

Acknowledgements

We are grateful to Prof. Ivano Bertini for his continuous advice and support. We thank Dr. Luisa Poggi for helpful discussions. S.B. is a Marie Curie Host Fellow Early Stage Research Training (EST) (Contract MEST-CT-2004-504391). B.J. is a Marie Curie Intra European Fellow (EIF) (Contract RTD-D5/AH D(2004)/528544). The project is funded by European Union, "Structural Proteomics IN Europe, SPINE" (Contract QLG2-CT-2002-00988).

References

Akke, M., Forsén, S. and Chazin, W.J. (1991) *J. Mol. Biol.*, **220**, 173–189.
Akke, M., Forsén, S. and Chazin, W.J. (1995) *J. Mol. Biol.*, **252**, 102–121.
Allegrozzi, M., Bertini, I., Janik, M.B.L., Lee, Y.-M., Liu, G. and Luchinat, C. (2000) *J. Am. Chem. Soc.*, **122**, 4154–4161.
Arnesano, F., Banci, L., Bertini, I., Felli, I.C., Luchinat, C. and Thompsett, A.R. (2003) *J. Am. Chem. Soc.*, **125**, 7200–7208.
Babini, E., Bertini, I., Capozzi, F., Felli, I.C., Lelli, M. and Luchinat, C. (2004) *J. Am. Chem. Soc.*, **126**, 10496–10497.
Banci, L., Bertini, I., Bren, K.L., Cremonini, M.A., Gray, H.B., Luchinat, C. and Turano, P. (1996) *J. Biol. Inorg. Chem.*, **1**, 117–126.
Banci, L., Bertini, I., Gori Savellini, G., Romagnoli, A., Turano, P., Cremonini, M.A., Luchinat, C. and Gray, H.B. (1997) *Proteins Struct. Funct. Genet.*, **29**, 68–76.
Bermel, W., Bertini, I., Duma, L., Emsley, L., Felli, I.C., Pierattelli, R. and Vasos, P.R. (2005a) *Angew. Chem. Int. Ed.*, **44**, 3089–3092.
Bermel, W., Bertini, I., Felli, I.C., Pierattelli, R. and Vasos, P.R. (2005b) *J. Magn. Reson.*, **172**, 324–328.
Bertini, I., Carrano, C.J., Luchinat, C., Piccioli, M. and Poggi, L. (2002a) *Biochemistry*, **41**, 5104–5111.
Bertini, I., Cavallaro, G., Cosenza, M., Kümmerle, R., Luchinat, C., Piccioli, M. and Poggi, L. (2002b) *J. Biomol. NMR*, **23**, 115–125.
Bertini, I., Couture, M.M.J., Donaire, A., Eltis, L.D., Felli, I.C., Luchinat, C., Piccioli, M. and Rosato, A. (1996) *Eur. J. Biochem.*, **241**, 440–452.
Bertini, I., Donaire, A., Jiménez, B., Luchinat, C., Parigi, G., Piccioli, M. and Poggi, L. (2001a) *J. Biomol. NMR*, **21**, 85–98.
Bertini, I., Duma, L., Felli, I.C., Fey, M., Luchinat, C., Pierattelli, R. and Vasos, P.R. (2004a) *Angew. Chem. Int. Ed.*, **43**, 2257–2259.
Bertini, I., Felli, I.C., Kümmerle, R., Moskau, D. and Pierattelli, R. (2004b) *J. Am. Chem. Soc.*, **126**, 464–465.
Bertini, I., Janik, M.B.L., Lee, Y.-M., Luchinat, C. and Rosato, A. (2001b) *J. Am. Chem. Soc.*, **123**, 4181–4188.
Bertini, I., Jiménez, B. and Piccioli, M. (2005) *J. Magn. Reson.*, **174**, 125–132.
Bertini, I., Lee, Y.-M., Luchinat, C., Piccioli, M. and Poggi, L. (2001c) *ChemBioChem*, **2**, 550–558.
Bertini, I., Luchinat, C. and Parigi, G. (2001d) *Solution NMR of Paramagnetic Molecules*, Elsevier, Amsterdam.
Bleaney, B. (1972) *J. Magn. Reson.*, **8**, 91–100.
Bodenhausen, G. and Ruben, D.J. (1980) *Chem. Phys. Lett.*, **69**, 185–188.
Brodin, P., Grundstrom, T., Hofmann, T., Drakenberg, T., Thulin, E. and Forsén, S. (1986) *Biochemistry*, **25**, 5371–5377.
Caillet-Saguy, C., Delepierre, M., Lecroisey, A., Bertini, I., Piccioli, M. and Turano, P. *J. Am. Chem. Soc.* in press.
Chazin, W.J., Kördel, J., Drakenberg, T., Thulin, E., Brodin, P., Grundstrom, T. and Forsén, S. (1989) *Proc. Natl. Acad. Sci. USA*, **86**, 2195–2198.
Déméné, H., Tsan, P., Gans, P. and Marion, D. (2000) *J. Phys. Chem. B*, **104**, 2559–2569.

Donaire, A., Jiménez, B., Moratal Mascarell, J.M., Hall, J.F. and Hasnain, S.S. (2001) *Biochemistry*, **40**, 837–846.
Donaire, A., Salgado, J. and Moratal, J.M. (1998) *Biochemistry*, **37**, 8659–8673.
Eccles, C., Güntert, P., Billeter, M. and Wüthrich, K. (1991) *J. Biomol. NMR*, **1**, 111–130.
Emsley, L. and Bodenhausen, G. (1992) *J. Magn. Reson.*, **97**, 135–148.
Gelis, I., Katsaros, N., Luchinat, C., Piccioli, M. and Poggi, L. (2003) *Eur. J. Biochem.*, **270**, 600–609.
Grzesiek, S. and Bax, A. (1992) *J. Am. Chem. Soc.*, **114**, 6291–6293.
Hus, J.C., Marion, D. and Blackledge, M. (2000) *J. Mol. Biol.*, **298**, 927–936.
Johansson, C., Brodin, P., Grundstrom, T., Thulin, E., Forsén, S. and Drakenberg, T. (1990) *Eur. J. Biochem.*, **187**, 455–460.
Kay, L.E., Ikura, M., Tschudin, R. and Bax, A. (1990) *J. Magn. Reson.*, **89**, 496–514.
Kay, L.E., Marion, D. and Bax, A. (1989) *J. Magn. Reson.*, **84**, 72–84.
Kördel, J., Skelton, N.J., Akke, M. and Chazin, W.J. (1993) *J. Mol. Biol.*, **231**, 711–734.
Kostic, M., Pochapsky, S.S. and Pochapsky, T.C. (2002) *J. Am. Chem. Soc.*, **124**, 9054–9055.
Kretsinger, R.H. (1980) *CRC Crit. Rev. Biochem.*, **8**, 119–174.
Kurland, R.J. and McGarvey, B.R. (1970) *J. Magn. Reson.*, **2**, 286–301.
Machonkin, T.E., Westler, W.M. and Markley, J.L. (2002) *J. Am. Chem. Soc.*, **124**, 3204–3205.
Machonkin, T.E., Westler, W.M. and Markley, J.L. (2004) *J. Am. Chem. Soc.*, **126**, 5413–5426.
Malmendal, A., Carlström, G., Hambraeus, C., Drakenberg, T., Forsén, S. and Akke, M. (1998) *Biochemistry*, **37**, 2586–2595.
Marion, D. and Wüthrich, K. (1983) *Biochem. Biophys. Res. Commun.*, **113**, 967–974.
McConnell, H.M. and Robertson, R.E. (1958) *J. Chem. Phys.*, **29**, 1361–1365.
Miller, A.F., Padmakumar, K., Sorkin, D.L., Karapetian, A. and Vance, C.K. (2003) *J. Inorg. Biochem.*, **93**, 71–83.
Shaka, A.J., Barker, P.B. and Freeman, R. (1985) *J. Magn. Reson.*, **64**, 547–552.
Shaka, A.J., Keeler, J. and Freeman, R. (1983) *J. Magn. Reson.*, **53**, 313–340.
Skelton, N.J., Kordel, J., Akke, M., Forsen, S. and Chazin, W.J. (1994) *Nat. Struct. Biol.*, **1**, 239–245.
Sorkin, D.L. and Miller, A.F. (2000) *J. Biomol. NMR*, **17**, 311–322.
Tolman, J.R., Flanagan, J.M., Kennedy, M.A. and Prestegard, J.H. (1995) *Proc. Natl. Acad. Sci. USA*, **92**, 9279–9283.
Vathyam, S., Byrd, R.A. and Miller, A.F. (2000) *Magn. Reson. Chem.*, **38**, 536–542.
Vila, A.J. and Fernández, C.O. (1996) *J. Am. Chem. Soc.*, **118**, 7291–7298.
Vogel, H.J., Drakenberg, T., Forsén, S., O'Neil, J.D. and Hofmann, T. (1985) *Biochemistry*, **24**, 3870–3876.
Wilkens, S.J., Xia, B., Weinhold, F., Markley, J.L. and Westler, W.M. (1998) *J. Am. Chem. Soc.*, **120**, 4806–4814.
Xia, B., Pikus, J.D., McClay, K., Steffan, R.J., Chae, Y.K., Westler, W.M., Markley, J.L. and Fox, D.J. (1999) *Biochemistry*, **38**, 727–739.